ACI STRUCTURAL JOURNAL TECHNICAL PAPER

Title no. 91-S42

High-Strength Concrete Elements Subjected to Shear

by Frank J. Vecchio, M. P. Collins, and Jim Aspiotis

Orthogonally reinforced panels, constructed of high-strength concrete, were tested under conditions of in-plane shear and normal loads. The reinforcement and loading conditions were such as to result in a concrete shear failure after yielding of the transverse reinforcement, but prior to yielding of the longitudinal reinforcement. The crack-associated damage effects observed in the compression response of the concrete, in these elements, was significant. Modifications to previously developed constitutive relations, reflecting increased deterioration in the strength and stiffness of high-strength concrete, were determined and incorporated into finite element analysis procedures. The revised constitutive models and analysis procedures were found to simulate accurately the behavior of the high-strength concrete panels.

Keywords: compression; **finite element method**; **high-strength concretes; shear tests**.

In the nonlinear finite element analysis of reinforced concrete structures, it is common to use constitutive models for concrete that are based on a smeared, rotating crack idealization. Moreover, it is often recognized that the compression response of the concrete in a cracked element is substantially different than that of plain concrete in uniaxial compression. The presence of large transverse strains in cracked, biaxially stressed concrete serves to decrease the strength and stiffness of the concrete in the direction of principal compression (in the ascending portion of the stress-strain response). A number of constitutive models reflecting this influence have been proposed[1-4] and adopted in finite element codes. These models were largely formulated on the basis of data derived from test specimens constructed of normal strength concrete.

It is generally acknowledged that the pattern of crack formation in high-strength concrete is significantly different from that seen with normal strength concrete. High-strength concrete tends to be more brittle, with cracks forming through the aggregates rather than around them. The result could be a smoother fracture plane with subsequently less aggregate interlock. It is believed that, as a result, the crack-related damage effect is more pronounced in higher strength concrete. Data from preliminary tests performed on panels tended to support this view, and modifications to the constitutive models were proposed accordingly.[5,6] Neglecting a more pronounced softening in cracked high-strength concrete, if indeed present, would result in unconservative estimates of structural response as determined by finite element codes using current models.

Given that the test data in this area was sparse, further experimental investigation was undertaken. Reinforced concrete panels constructed using high-strength concrete were tested under various conditions of in-plane stress. Thus, the objectives were two-fold: 1) to provide a check on the accuracy of currently available constitutive models and finite element procedures in simulating high-strength concrete response; and 2) provide data for formulating improved models, if necessary. The details and results of the test program are discussed herein.

RESEARCH SIGNIFICANCE

This paper provides new test data pertaining to the behavior of high-strength reinforced concrete elements. The data is useful for developing constitutive models for compression response, and for corroborating analytical procedures.

EXPERIMENTAL PROGRAM

The experimental program involved the testing of 12 orthogonally reinforced panels constructed of high-strength concrete. The panels were subjected to monotonic, proportional loads with various combinations of in-plane shear and biaxial stress.

The test panels were 890 x 890 mm (35 in.) in plan dimension, with a thickness of 70 mm (2.75 in.). Typically, the panels were orthogonally reinforced with one or two layers of deformed bars in each direction. The reinforcement in the longitudinal direction (i.e., x-direction) was generally heavier than that in the transverse direction (i.e., y-direction). To insure adequate load transfer in the transverse direction, additional anchorage reinforcement was provided at the loading keys. No out-of-plane reinforcement was used. Details pertaining to the panels' construction are shown in Fig. 1(a);

ACI Structural Journal, V. 91, No. 4 July-August 1994.

Received Feb. 15, 1993, and reviewed under Institute publication policies. Pertinent discussion will be published in the May-June 1995 *ACI Structural Journal* if received by Jan. 1, 1995.

ACI member ***Frank J. Vecchio*** *is an associate professor of civil engineering at the University of Toronto, Ontario, Canada. A member of ACI Committee 435, Deflections of Structures, and 447, Finite Element Analysis, his research interests relate primarily to the constitutive modeling, nonlinear analysis, and computer-aided design of reinforced concrete.*

M. P. Collins, *FACI, is a professor of civil engineering at the University of Toronto. He is a member of joint ACI-ASCE Committee 445, Shear and Torsion, and ACI Committee 358, Concrete Guideways, and has coauthored a textbook on prestressed concrete basics and written numerous technical papers on structural concrete. Among other distinctions, he was a corecipient of ACI's Raymond C. Reese Research Medal in 1976.*

Jim Aspiotis *is a graduate of the University of Toronto, earning an MASc degree in structural concrete. He is a design engineer with Yolles Ltd., Consulting Engineers, Toronto.*

specimen test parameters are given in Table 1. Note that the primary variables were percentage of transverse reinforcement and loading conditions.

The nominal compressive strength of the concrete used to construct the panels was 55 MPa (8.0 ksi); actually, strengths ranged from 43 to 72 MPa (6.2 to 10.4 ksi). The concrete for each panel was hand-batched using Type 10 portland cement and 10-mm ($^3/_8$-in.) crushed limestone. A superplasticizer was also used to improve the workability of the mix. The panels and test cylinders were sealed and cured for 5 to 7 days, and tested at approximately 14 to 21 days of age.

The properties of the concrete, determined from cylinders tested at the time of the panel tests, are listed in Table 1. A typical compressive stress-strain curve, determined using a stiff deformation-controlled universal test machine, is given in Fig. 2(a).

The deformed reinforcement bars were heat-treated [typically 2 hr at 675 C (1250 F)] to produce a flat yield plateau. The mechanical properties of the reinforcing steel, determined from coupon tests, are listed in Table 1. Typical tension stress-strain response curves are shown in Fig. 2(b).

During testing, specimen deformations were continuously monitored using LVDTs placed on both faces of the panel. They were arranged to measure average strains in the x- and y-reinforcement directions, and in the two diagonal directions. Also, mechanical strain gage measurements were made in the longitudinal, transverse, and diagonal directions, on both sides, using 200-mm base-length 16-point grids [see Fig. 1(b)]. Applied loads were determined from the hydraulic pressures fed to the previously calibrated loading jacks. Several of the jacks were equipped with load cells to provide a check on the calculated loads.

Uniform in-plane forces were applied to the panels using the shear rig test facility [see Fig. 1(c) and (d)]. The facility is comprised of a self-reacting frame containing 40 double-acting 210-kN- (47-kip)-capacity hydraulic jacks, controlled by a six-channel pressure-proportioning/maintaining device. The applied loads in each test, in the proportions given in Table 1, were monotonically increased until the specimen failed. At several discrete load stages, loading was momentarily halted while the various measurements were taken. Typically, 12 to 15 load stages were employed over the course of a test.

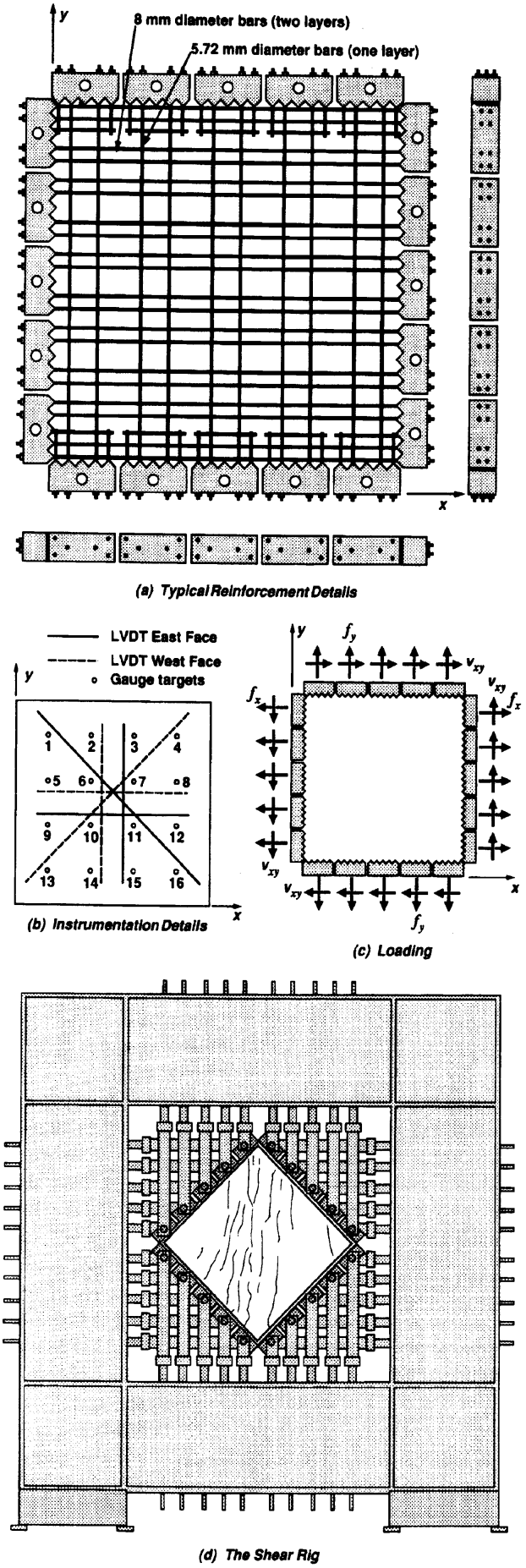

Fig. 1—Test specimen details: (a) reinforcement; (b) instrumentation; (c) loading; (d) test rig (25.4 mm = 1 in.)

Table 1—Specimen details and loading conditions

	Concrete			Reinforcement				Loading
	f'_c, MPa	$\varepsilon_0 \times 10^{-3}$	f'_t, MPa	ρ_x, percent	f_{yx}, MPa	ρ_y, percent	f_{yy}, MPa	f_n/V, MPa
PHS1	72.2	-2.68	3.11	3.23	606	0.00	521	0.00
PHS2	66.1	-2.48	2.39	3.23	606	0.41	521	0.00
PHS3	58.4	-2.44	2.63	3.23	606	0.82	521	0.00
PHS4	68.5	-2.60	2.82	3.23	606	0.82	521	+0.25
PHS5	52.1	-2.58	1.99	3.23	606	0.41	521	0.25
PHS6	49.7	-2.25	2.06	3.23	606	0.41	521	-0.25
PHS7	53.6	-2.10	2.61	3.23	606	0.82	521	-0.25
PHS8	55.9	-2.17	2.59	3.23	606	1.24	521	0.00
PHS9	56.0	-2.68	2.42	3.23	606	0.41	521	-0.25
PHS10	51.4	-2.45	3.01	3.23	606	1.24	521	+0.25
PA1	49.9	-2.09	3.09	1.65	522	0.82	522	0.00
PA2	43.0	-1.99	2.91	1.65	522	0.82	522	0.00

6.90 MPa = 1 ksi

TEST RESULTS

The amount of reinforcement and the proportion of normal to shear load were factors found to significantly influence the panels' ultimate strength, failure mode, cracking, and ductility. These observations will be discussed herein. A summary of pertinent test results is given in Table 2. Shear load-deformation responses are given in Fig. 3.

Six of the panels were tested in pure shear (PHS1, PHS2, PHS3, PHS8, PA1, and PA2). In each of the two series (PHS and PA), the concrete strength and percentage of longitudinal reinforcement were relatively constant while the amount of transverse reinforcement was varied. The amount of longitudinal reinforcement provided in the PA-series elements was approximately half that provided in the PHS-series panels.

In all pure shear tests, the initial cracks in the elements developed at an angle of slightly less than 45 deg to the transverse reinforcement direction. First cracking occurred at shear stresses of about $0.3\sqrt{f_c'}$ MPa ($4\sqrt{f_c'}$ psi). In the more heavily reinforced panels, the cracks that developed subsequently were generally finer in width and more closely spaced. After yielding of the transverse reinforcement, a noticeable reorientation of the crack direction was seen as the cracks became more acute to the longitudinal reinforcement direction (i.e., x-direction). The rotation of cracks was most apparent in the elements with light transverse reinforcement (i.e., Panels PHS2 and PHS3).

The mode of failure observed in the pure shear tests was one involving a sliding shear failure of the concrete after yielding of the transverse reinforcement. The plane of failure was always parallel to the longitudinal reinforcement, and was accompanied by severe crushing and spalling of the concrete. In no case did the longitudinal reinforcement yield. Typically, the load-deformation responses were very ductile [see Fig. 3(a) and (b)]. As would be expected, the elements more heavily reinforced in the transverse direction exhibited greater stiffness and ultimate shear strength.

The PA-series panels with less longitudinal reinforcement were somewhat less ductile than the PHS-series elements. The failure mode was unchanged, however, with the concrete shear failure occurring almost immediately after yielding of the transverse reinforcement. Localized yielding of the longitudinal reinforcement may have accompanied the concrete failure, however. Crack reorientation was not as noticeable in these tests.

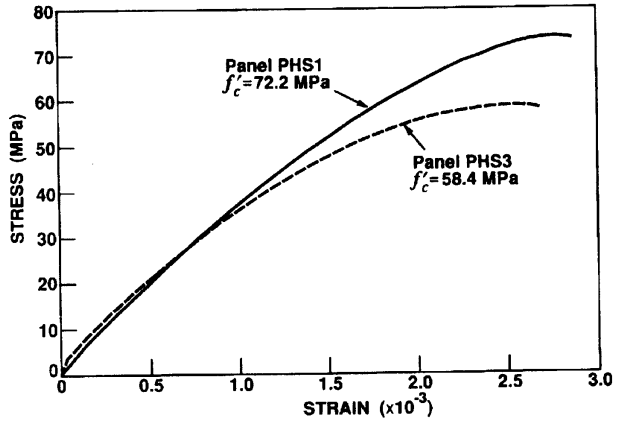

(a) Typical Concrete Cylinder Stress-Strain Curves

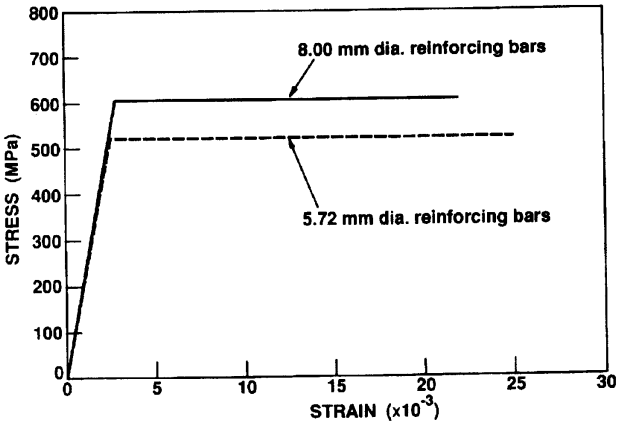

(b) Typical Reinforcement Stress-Strain Curves

Fig. 2—Material properties: (a) typical cylinder compression response; (b) typical reinforcement tension response (6.90 MPa = 1 ksi; 25.4 mm = 1 in.)

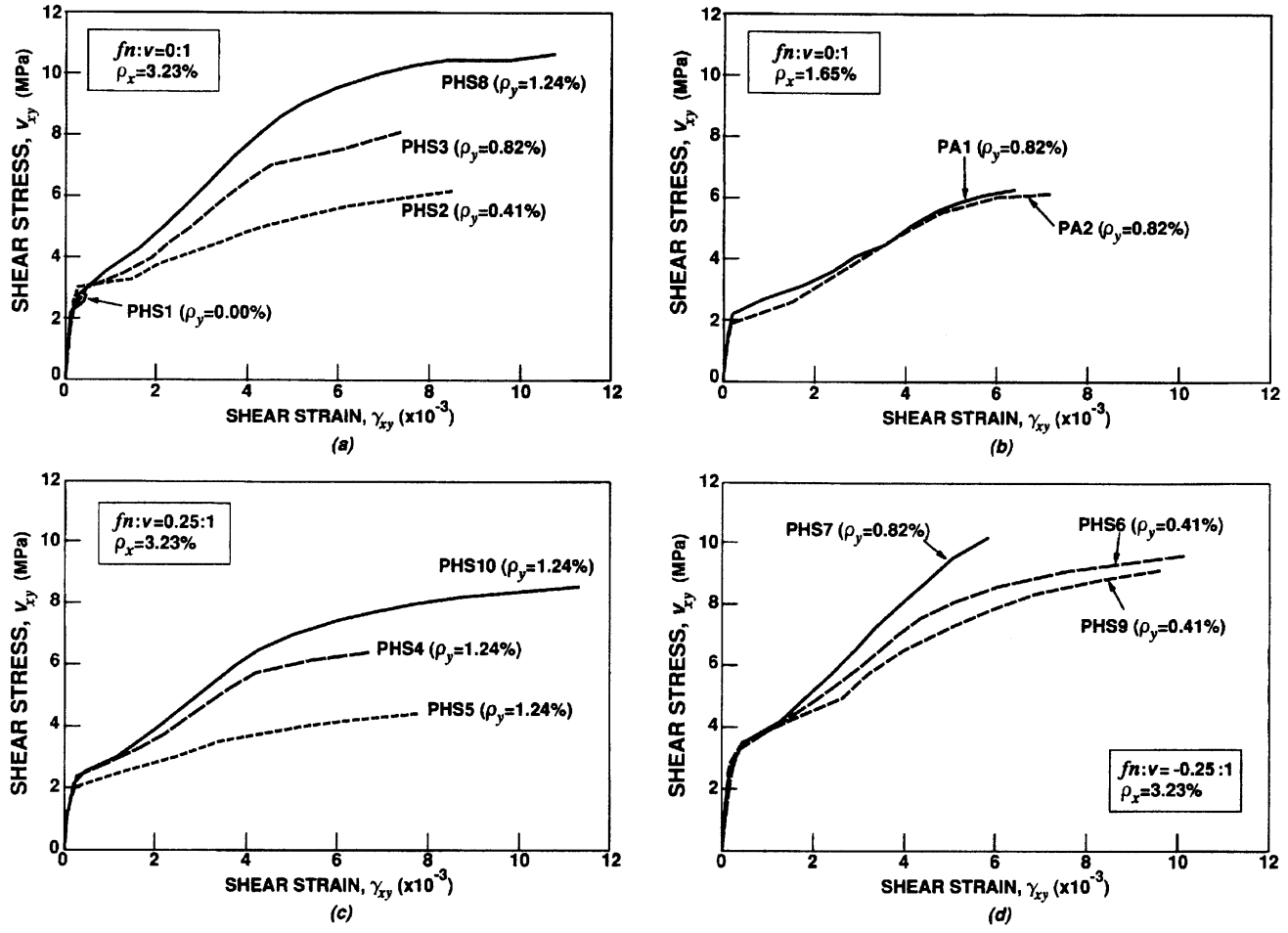

Fig. 3—Measured shear deformation responses: (a) PHS panels in pure shear; (b) PA panels in pure shear; (c) panels in biaxial tension and shear; (d) panels in biaxial compression and shear (6.90 MPa = 1 ksi)

Table 2—Test results

	f_n/V, MPa	V_{cr}, MPa	V_{yy}, MPa	V_u, MPa	ε_{xu} x 10^{-3}	ε_{yu} x 10^{-3}	γ_{xyu} x 10^{-3}	ε_{1u} x 10^{-3}	ε_{2u} x 10^{-3}	f_{c2u}, MPa	Failure mode
PHS1	0.00	2.54	—	2.95	0.09	0.11	0.34	0.27	-0.07	-3.31	CSS
PHS2	0.00	1.94	4.84	6.66	2.16	16.28	8.51	10.06	-0.70	-17.85	CST
PHS3	0.00	2.28	6.98	8.19	1.57	5.53	9.13	8.53	-0.73	-16.65	CST
PHS4	+0.25	2.39	5.76	6.91	1.82	11.07	9.42	13.04	-0.43	-14.85	CST
PHS5	+0.25	1.62	3.53	4.81	1.41	13.93	10.74	15.91	-0.71	-10.93	CST
PHS6	-0.25	2.25	7.30	9.89	1.76	9.64	10.78	12.37	-1.41	-21.08	CST
PHS7	-0.25	2.25	9.56	10.26	1.37	3.10	6.93	5.79	-0.77	-19.92	CST
PHS8	0.00	2.15	8.87	10.84	2.39	9.88	13.15	13.70	-1.43	-23.55	CST
PHS9	-0.25	2.22	6.57	9.37	1.73	9.47	11.16	12.39	-1.19	-20.19	CST
PHS10	+0.25	2.13	6.93	8.58	2.08	7.93	11.34	11.02	-1.34	-17.83	CST
PA1	0.00	2.19	6.29	6.34	2.23	4.13	7.12	6.87	-0.51	-11.83	CST
PA2	0.00	1.88	5.97	6.22	2.16	4.68	7.62*	7.43*	-0.59*	-11.79	CST

* Strain measurements determined from last Zurich load stage.
Note: CST = concrete shear crushing failure after transverse reinforcement has yielded; CSS = concrete shear-sliding failure.
6.90 MPa = 1 ksi.

Specimen PHS1, with no transverse reinforcement, failed almost immediately after first cracking. Cracking was more concentrated, and rotation of cracks was not apparent.

Three of the panels were subjected to biaxial tension and shear loads (PHS4, PHS5, and PHS10). The ratio of normal to shear stresses f_n/v remained fixed at 0.25 while the loads were increased monotonically. The behavior of these elements was similar, in many respects, to that of the pure shear elements. Cracks initially developed at slightly less than 45 deg to the transverse direction [see Fig. 4 (a)], and became more acute to the longitudinal direction after the transverse reinforcement yielded [see Fig. 4 (b)]. Cracking was more pronounced, however, compared to the pure shear elements; the average crack widths were larger, and the average crack spacings were smaller. Again, the failure mode involved a brittle shear/crushing failure of the concrete after the reinforcement in the transverse direction had yielded [see Fig. 4 (c)]. The presence of the biaxial tension reduced the shear stiffness of the panels, and caused a lowering of the ultimate shear strength by an average of 22 percent [see Fig. 3(c)].

Three of the panels (PHS6, PHS7, and PHS9) were tested under biaxial compression and shear, at a fixed f_n/v-ratio of -0.25. Relative to the pure shear specimens, the presence of the biaxial compressive stresses resulted in an elevated cracking stress, fewer visible cracks prior to failure, smaller crack widths, and a stiffer load-deformation response [see Fig. 3(d)]. Most significantly, the ultimate shear capacity of the panels was increased by an average of 38 percent. All three panels were characterized by an explosive concrete crushing failure, parallel to the longitudinal reinforcement, occurring after yield of the transverse reinforcement. Crack reorientations were not noticeable prior to failure.

To test the repeatability of results, Panels PHS6 and PHS9 were designed as duplicate specimens. The reinforcement properties and loading conditions were identical, and the concrete strengths were fairly similar [50 MPa (7.25 ksi) in PHS6; 56 MPa (8.12 ksi) in PHS9]. The cracking patterns, load-deformation responses, and failure modes observed for the two panels were very much alike (see Fig. 5). The average measured shear stress at maximum load for panels of PHS6 was 9.89 MPa (1.43 ksi); that for PHS9 was 5 percent lower at 9.37 MPa (1.36 ksi). [It should be mentioned that the test cylinders cast for PHS6 contained many voids (the panel itself did not). Thus, the strength of the concrete in PHS6 was likely higher than measured.]

MODIFICATION TO SOFTENING MODELS

Cracked reinforced concrete in compression has been observed to exhibit lower strength and stiffness than uniaxially compressed concrete. This degradation is primarily related to the degree of transverse straining and cracking present in the concrete. The softening effect may be more pronounced in high-strength concrete.

Analytical models for describing the softening effect were derived from test data,[1,2] and were recently updated.* Generally, two variations in the softening model exist: one where the compression base curve is modified in terms of both the peak stress attainable and the strain at which the peak stress

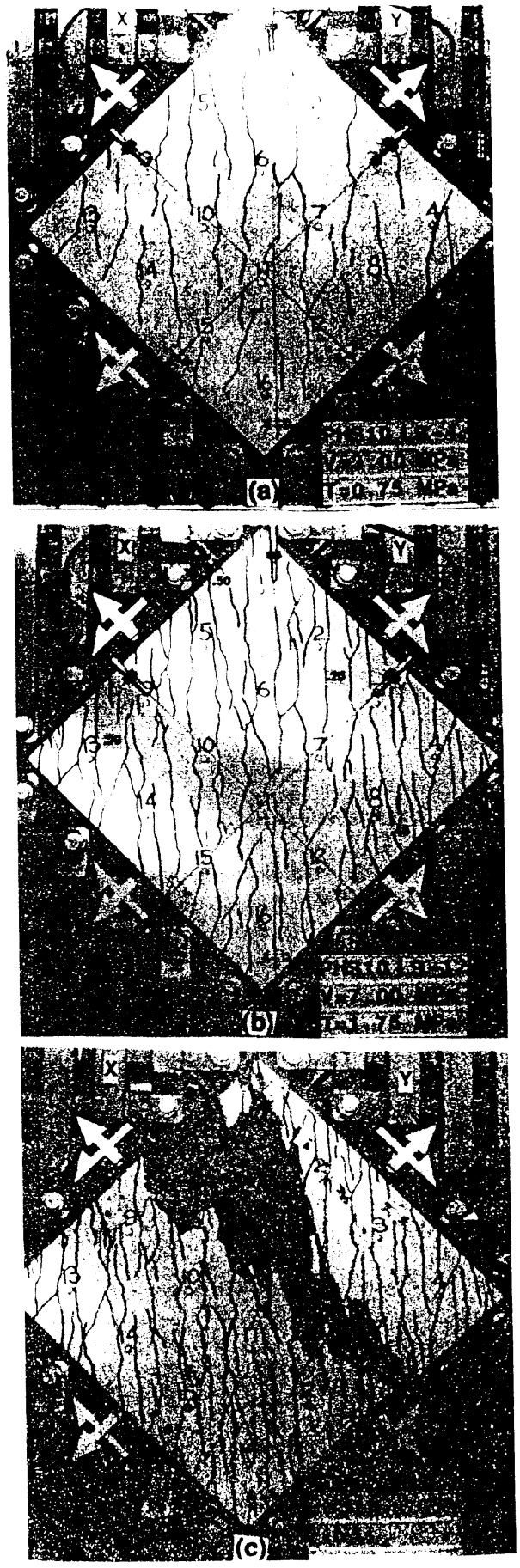

Fig. 4—Photos of Panel PHS10 during testing: (a) after cracking; (b) after yielding of transverse reinforcement; (c) after shear failure of concrete

*Vecchio, F. J., and Collins, M. P., "Compression Response of Cracked Reinforced Concrete," *Journal of Structural Engineering*, ASCE, in press.

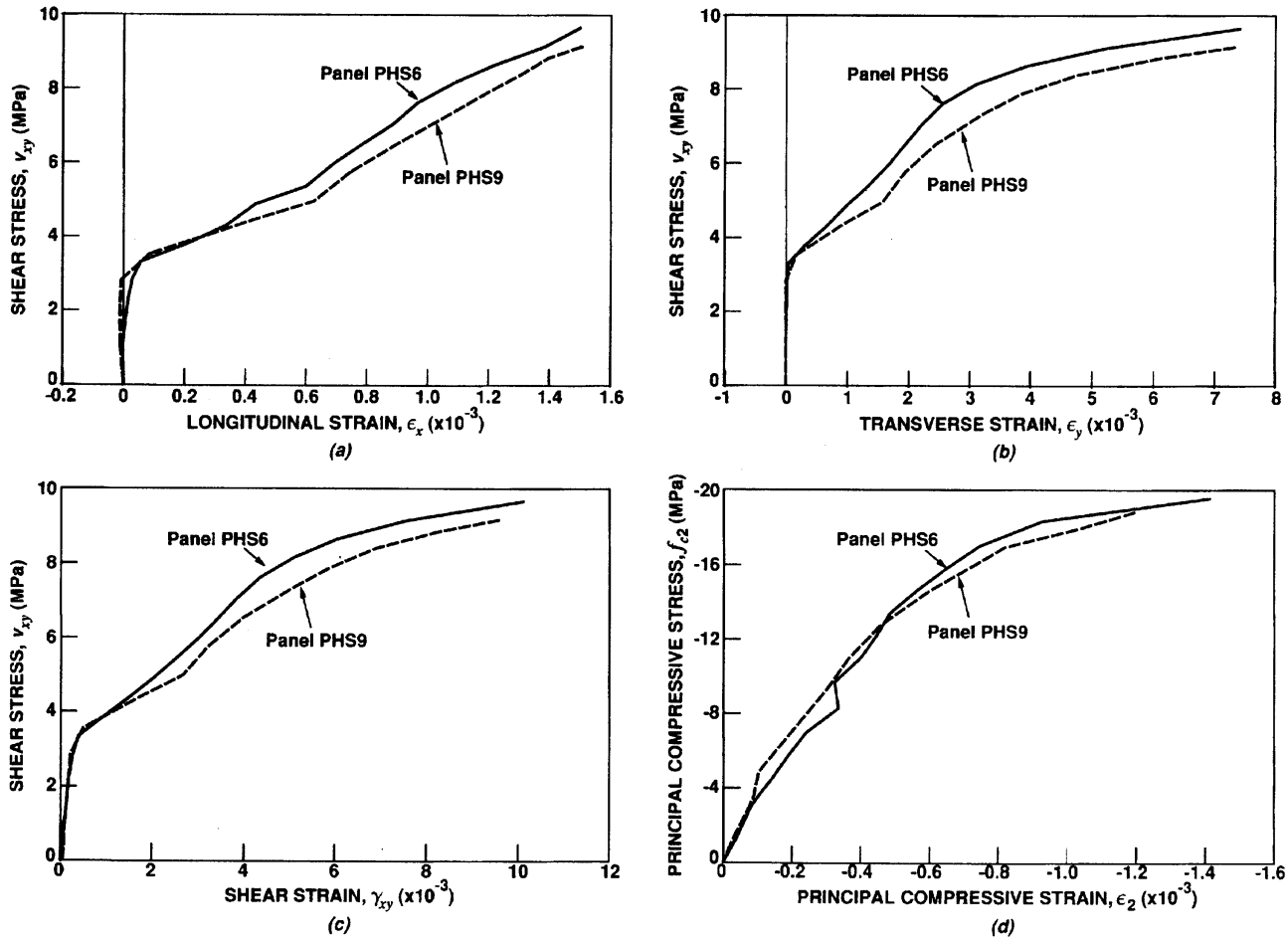

Fig. 5—Comparison of companion specimens PHS6 and PHS9 (6.90 MPa = 1 ksi)

occurs [see Fig. 6(a)]; and one where the base curve is modified in terms of the peak stress only [see Fig. 6(b)]. In both cases, the modification factor takes the form

$$\beta = \frac{1}{1 + K_c K_f} \tag{1}$$

where K_c represents the effect of the transverse cracking and straining, and K_f represents the dependence on the strength of the concrete f'_c. In both cases, the base curve used is that originally suggested by Thorenfeldt, Tomaszewicz, and Jensen,[7] and later calibrated by Collins and Porasz.[5]

In the strength and strain-softened model [Model A, Fig. 6(a)], the influence of the transverse strain is represented by

$$K_c = 0.35\,(-\varepsilon_1/\varepsilon_2 - 0.28)^{0.80} \tag{2}$$

where ε_1 is the average principal tensile strain and ε_2 is the average principal compressive strain.* In the strength-only softened model [Model B, Fig. 6(b)], the modification factor is

$$K_c = 0.27\,(\varepsilon_1/\varepsilon_0 - 0.37) \tag{3}$$

where ε_0 is the strain at peak cylinder stress. The strength and strain-softened model is somewhat more complex, but gives appreciably more accurate predictions. Full details are discussed elsewhere.

Two prime objectives in undertaking the test program previously described were to confirm the validity of the softening models for high-strength concrete, and determine the strength-influence factor K_f. The test data derived from this, and previous, series of panel tests were thus examined for dependence on concrete strength. Plotted in Fig. 7 are the experimentally determined principal compressive stresses $f_{c2\text{-}exp}$ against the concrete cylinder strengths (f'_c). The experimental compressive stresses were normalized relative to stresses calculated from the base curve [Fig. 7(a)], and relative to stresses calculated from Model A [Fig. 7(b)] and Model B [Fig. 7(c)]. A slight dependence on f'_c can be seen in these plots, although the correlation is weak and the scatter is large.

*Vecchio, F. J., and Collins, M. P., "Compression Response of Cracked Reinforced Concrete," *Journal of Structural Engineering*, ASCE, V. 119, No. 12, Dec. 1993, pp. 3590-3610.

*Vecchio, F. J., and Collins, M. P., "Compression Response of Cracked Reinforced Concrete," *Journal of Structural Engineering*, ASCE, V. 119, No. 12, Dec. 1993, pp. 3590-3610

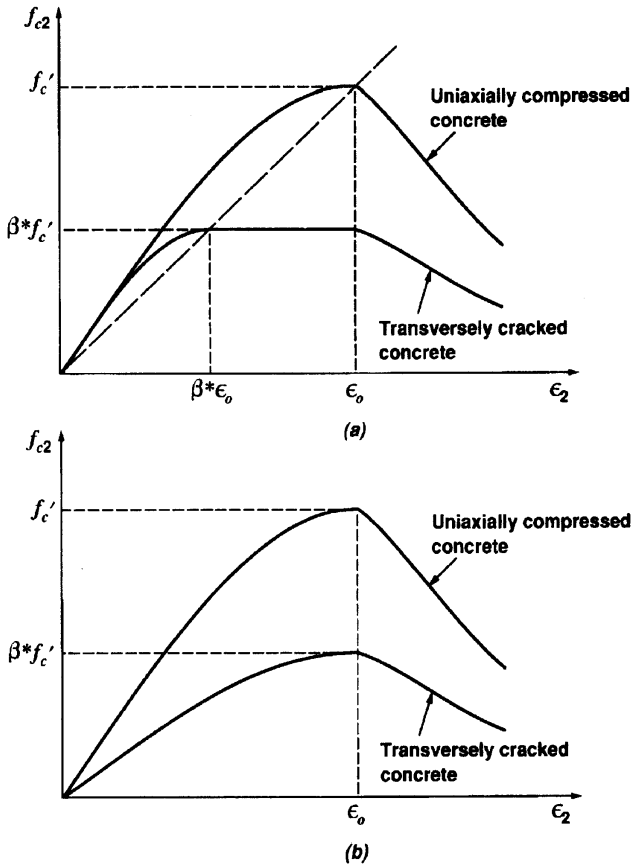

Fig. 6—Compression response models: (a) Model A, peak stress and peak strain reduced; (b) Model B, peak stress only reduced

Table 3—Correlation of principal compressive stresses

Model	$f_{c2\text{-experimental}} / f_{c2\text{-theoretical}}$					
	All panel test series			PHS and PA series		
	Mean	Standard deviation	Coefficient of variation, percent	Mean	Standard deviation	Coefficient of variation, percent
Model A, without K_f	0.97	0.19	19.57	0.90	0.11	12.58
Model A, with K_f	1.00	0.19	18.85	0.98	0.15	15.69
Model B, without K_f	1.02	0.22	21.11	1.14	0.15	12.78
Model B, with K_f	1.00	0.22	22.25	1.01	0.12	11.76

For Model A [Fig. 6(a); Eq. (1) and (2)], a statistical examination of the data produced the following expression for the K_f factor

$$K_f = 0.1825 \sqrt{f_c'(MPa)} \geq 1.0 \quad (4)$$

For Model B [Fig. 6(b); Eq. (1) and (3)], the K_f factor was determined as

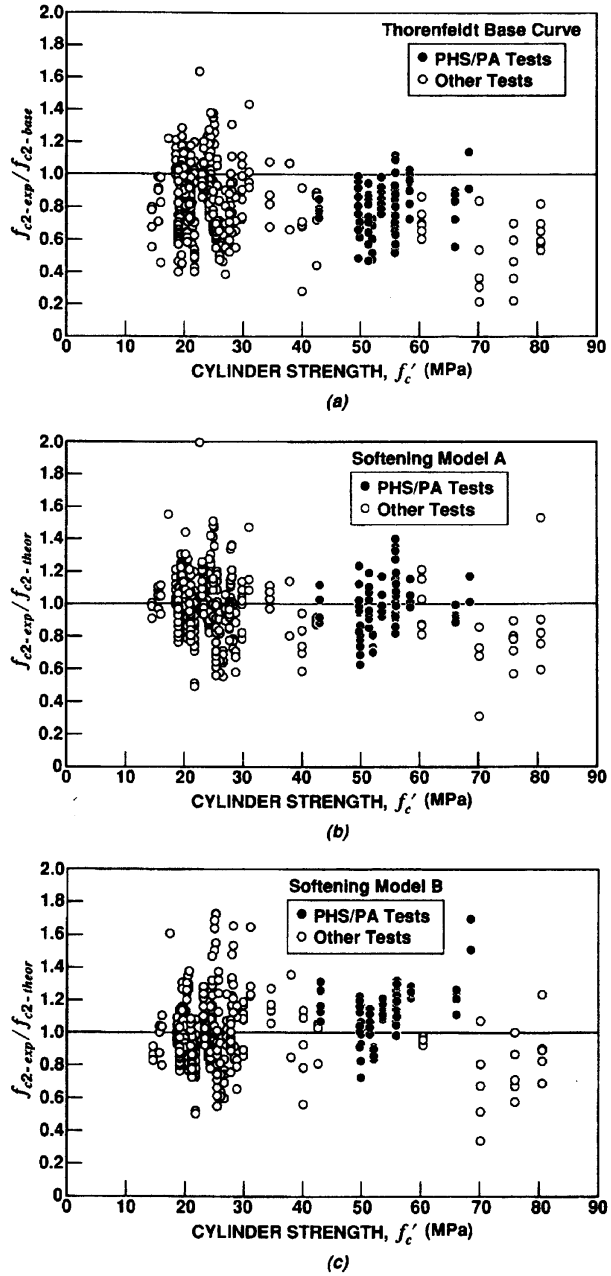

Fig. 7—Dependence of compression-softening on concrete strength: (a) using Thorenfeldt base curve; (b) using softening model A; c) using softening model B (6.90 MPa = 1 ksi)

$$K_f = 2.55 - 0.2629 \sqrt{f_c'(MPa)} \leq 1.11 \quad (5)$$

From Table 3, it can be seen that the inclusion of the K_f factor results in a small but definite improvement in the accuracy of the analytical models.

FINITE ELEMENT ANALYSIS

The modifications to the compression models were incorporated into the nonlinear finite element program TRIX.[8] Analyses were then undertaken to determine the theoretical behavior of each of the test panels.

Table 4—Finite element analysis results

	$V_{u\text{-experimental}} / V_{u\text{-theoretical}}$			
	Model A	Model B	Model A, without K_f	No softening
PHS1	0.95	0.99	0.95	0.95
PHS2	1.01	0.99	0.98	0.98
PHS3	0.91	0.88	0.88	0.88
PHS4	0.99	0.99	0.99	0.99
PHS5	1.09	1.06	1.07	1.02
PHS6	1.13	1.08	1.07	0.95
PHS7	0.89	0.84	0.84	0.77
PHS8	1.00	0.96	0.96	0.96
PHS9	1.03	1.04	0.95	0.90
PHS10	1.00	0.98	0.98	0.98
PA1	1.02	1.02	1.02	1.03
PA2	1.00	1.00	1.00	1.00
Mean	1.00	0.99	0.98	0.95
Coefficient of variation, percent	6.55	7.00	6.90	7.40

The test panels were of homogeneous construction, with evenly distributed reinforcement, and subjected to uniform loads. Hence, a finite element mesh consisting of a single rectangular element was sufficient in modeling the panels. The concrete and reinforcement material properties used were as determined from the test cylinders and coupons (see Table 1). Poisson's ratio for concrete was assumed to be 0.15. Small increments in load were applied until the ultimate load capacities of the panels were achieved.

Table 4 compares the predicted and observed failure loads for each of the panels. Excellent correlation was attained with each of the theoretical models. Using the model in which both the peak compressive stress and peak strain are modified (Model A), the ratio of the experimental to theoretical shear strength had a mean of 1.00 and a coefficient of variation of 6.55 percent. With the model in which the peak strength only is modified (Model B), the correlation was almost equally good (mean, 0.99; coefficient of variation, 7.00 percent). Both models predicted that all PHS-series panels would experience a shear failure of the concrete after yielding of the transverse reinforcement, but prior to yielding of the longitudinal reinforcement. For the PA-series panels, the analyses suggested that the concrete failure would be accompanied by local yielding of the longitudinal reinforcement at the crack locations. These predictions were consistent with the experimentally observed behavior. (Recall that the test cylinders for Panel PHS6 were poorly cast, likely producing a low estimate of the strength of the concrete in that panel and thus leading to the low theoretical shear strength predicted.)

The load-deformation responses of the test panels were also simulated with very good accuracy. Shown in Fig. 8 are the shear deformation responses for three representative panels: PHS8, loaded in pure shear; PHS9, loaded in combined biaxial compression and shear; and PHS10, loaded in combined biaxial tension and shear. In general, there was close agreement between predicted and observed response at all stages of loading. However, there was a tendency to slightly overestimate ductility after yielding of the reinforcement. Equally good correlation was achieved with respect to strains in the longitudinal and transverse reinforcement directions.

Shown in Fig. 9 are the concrete principal compressive stress-strain responses, determined using the two models, for the three representative panels. Also shown are the experimentally determined responses. In general, the correlation of the predicted responses to the test data was at a satisfactory level. Note, however, that Model B tended to underestimate stiffness initially, and then overestimate stiffness near ultimate load. Model A provided generally more accurate correlation with the test data at all stages of loading.

To get an indication of the significance of including the concrete strength-dependent modification factor K_f [Eq. (4)], the panels were reanalyzed with the factor omitted. The influence on the computed ultimate shear strength of the panels was slight, with the ratio of experimental to theoretical shear strength changing to a mean value of 0.98 and a coefficient of variation of 6.90 percent (see Table 4). The influence on the overall shear deformation response was, in general, also slight [see Fig. 10(a)]. The effect of the response in the principal compressive direction was somewhat more substantial, however, with the concrete exhibiting greater strength and stiffness [see Fig. 10(b)].

Finally, to investigate the importance of including a compression-softening model, the panels were reanalyzed with the stress- and strain-reduction factor β [Eq. (1) and (2)] omitted. The predicted strength of the panels rose by an average of 5.0 percent, with a slight deterioration in the coefficient of variation (see Table 4). More importantly, however, the predicted failure mode changed, in all panels, to one involving a ductile yielding of both the longitudinal and transverse reinforcement with no crushing of the concrete. Also, the stiffness of the shear deformation response, and of the concrete compressive stress-strain response, were significantly overestimated (see Fig. 10). Thus, ignoring the compression-softening effect resulted in a significant misjudgment of the behavior of the panels despite not changing the failure load much.

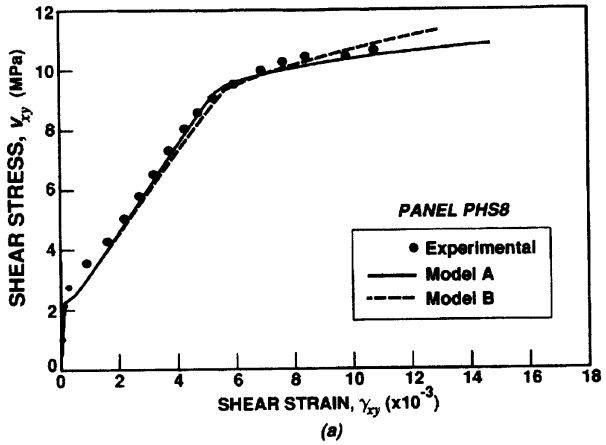

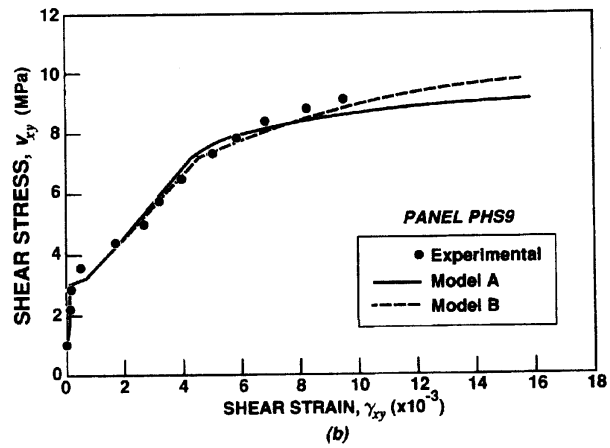

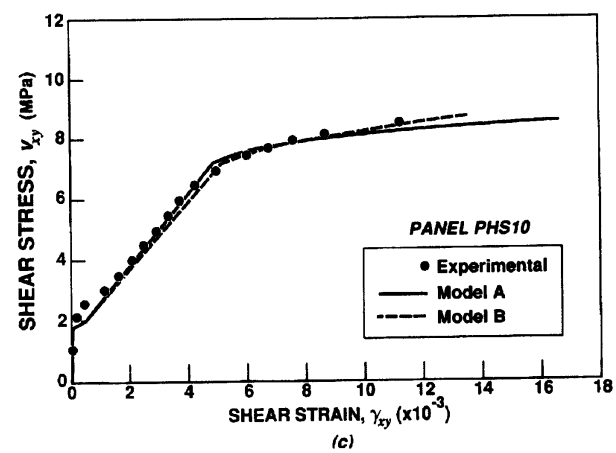

Fig. 8—Comparison of experimental and theoretical shear deformation response: (a) Panel PHS8; (b) Panel PHS9; (c) Panel PHS10 (6.90 MPa = 1 ksi)

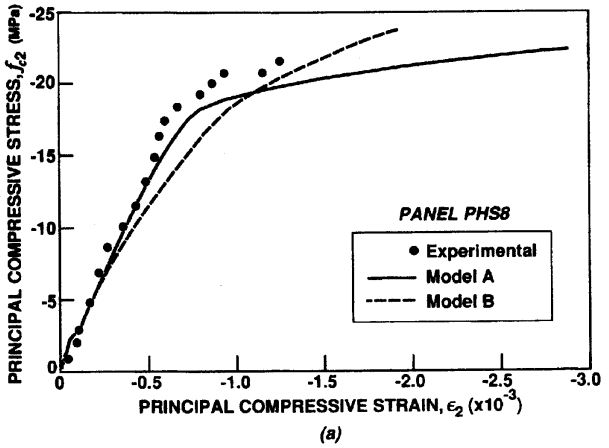

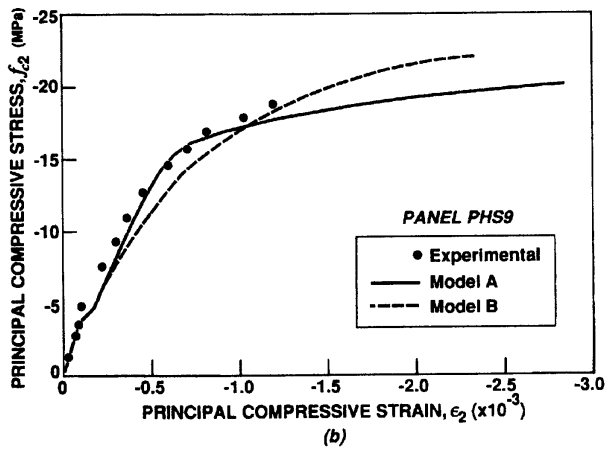

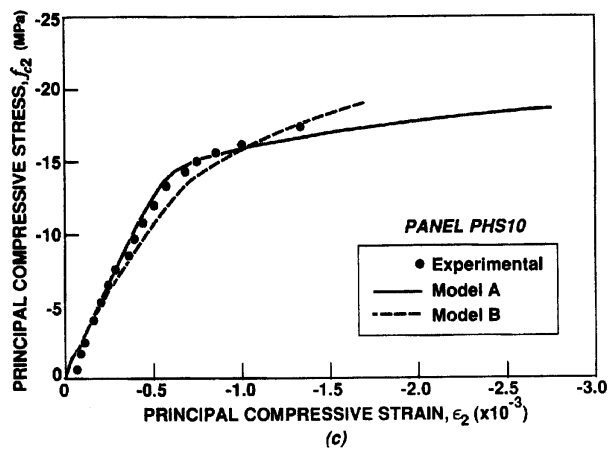

Fig. 9—Comparison of experimental and theoretical concrete principal compressive stress-strain response: (a) Panel PHS8; (b) Panel PHS9; (c) Panel PHS10

CONCLUSIONS

Twelve orthogonally reinforced high-strength concrete panels were tested under combinations of in-plane shear and normal stress. The nominal strength of the concrete used was 55 MPa (8.0 ksi).

The panels exhibited ductile load-deformation responses. The failure model at ultimate load typically involved crushing of the concrete, occurring after yielding of the transverse reinforcement but prior to yielding of the longitudinal reinforcement. After yielding of the transverse reinforcement, a gradual reorientation of cracks was observed. Cracking, and ultimate load capacity, were highly influenced by the presence of normal stresses.

The principal compressive stress response of the concrete in the panels, and the crack-associated degradation effects, were examined. The constitutive models previously developed for normal strength concrete were found to simulate accurately the responses observed in this test series. The constitutive model in which both the peak stress and peak strain parameters are modified gave somewhat better correlation to the test data than did the model in which only the peak stress is modified. A slightly increased degree of soft-

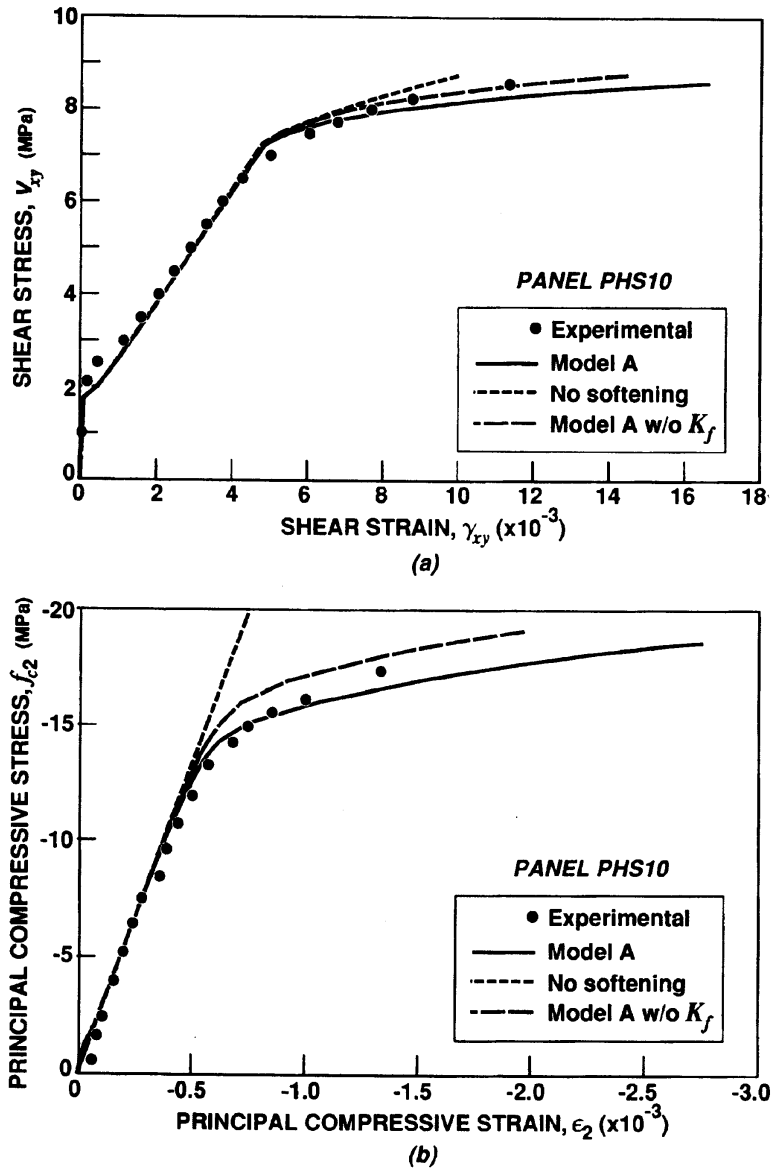

Fig. 10—Influence of strain-softening formulations: (a) shear stress-strain response of Panel PHS10; (b) principal compression response of Panel PHS10

ening was found to develop in high-strength concrete. Formulations describing this effect were found and incorporated into the constitutive models.

Finite element analyses, when including the compression-softening models and the concrete strength-dependent modification factors, gave theoretical responses that correlated well with the experimentally observed behavior. The panels' strength, failure mode, and deformation responses were modeled accurately. The strength and strain-softened model again gave slightly better results than the strength-only softening model. Ignoring the concrete strength-dependent factor, K_f produced a slight deterioration in the accuracy of the theoretical responses. Ignoring the softening factor β resulted in incorrectly predicted failure modes and significantly overestimated panel strengths and stiffnesses.

In general, the compression-softening formulations and analysis procedures previously developed for normal strength concrete elements were found to apply equally well to high-strength concrete elements.

ACKNOWLEDGMENT

The work described in this paper was funded by a Strategic Grant from the Natural Sciences and Engineering Research Council of Canada and by the Networks of Centres of Excellence for High Performance Concrete. The authors are appreciative of the support received.

NOTATION

f_{c2} = principal compressive stress in concrete
f_n = normal stress applied to panel in x- and y-directions
f_x = normal stress applied to panel in x-direction
f_y = normal stress applied to panel in y-direction
f_{yx} = yield stress of x-direction reinforcement
f_{yy} = yield stress of y-direction reinforcement
f_c' = nominal compressive strength of concrete
f_c' = tensile strength of concrete
K_c = transverse strain-related modification factor
K_f = concrete strength-related modification factor
v = shear stress applied to panels
v_{cr} = shear stress at first cracking
v_{yy} = shear stress at first yielding of transverse reinforcement
v_u = ultimate shear capacity of panel
β = compression-softening factor
ε_1 = average principal tensile strain
ε_2 = average principal compressive strain
ε_0 = strain at peak compressive stress in cylinder
ε_x = average strain in x-direction
ε_y = average strain in y-direction
γ_{xy} = average shear strain relative to x- and y-axes
ρ_x = x-direction reinforcement ratio
ρ_y = y-direction reinforcement ratio

REFERENCES

1. Vecchio, F. J., and Collins, M. P., "Response of Reinforced Concrete to In-Plane Shear and Normal Stresses," *Publication* No. 82-03, Department of Civil Engineering, University of Toronto, Mar. 1982, 332 pp.

2. Vecchio, F. J., and Collins, M. P., "Modified Compression-Field Theory for Reinforced Concrete Elements Subjected to Shear," ACI JOURNAL, V. 83, No. 2, Mar.-Apr. 1986, pp. 219-231.

3. Miyahara, T.; Kawakimi, T.; and Maekawa, K., "Nonlinear Behaviour of Cracked Reinforced Concrete Plate Element under Uniaxial Compression," *Concrete Library International,* JSCE, No. 11, 1988, pp. 306-319.

4. Belarbi, A., and Hsu, T. T. C., "Constitutive Laws of Reinforced Concrete in Biaxial Tension-Compression," University of Houston, *Research Report* UHCEE 91-2, 1991, 155 pp.

5. Collins, M. P., and Porasz, A., "Shear Strength for High Strength Concrete," *Bulletin d'Information No. 193—Design Aspects of High Strength Concrete,* CEB, 1989, pp. 75-83.

6. Ueda, M.; Noguchi, H.; Shirai, N.; and Morita, S., "Introduction to Activity of New RC," *Proceedings,* International Workshop on Finite Element Analysis of Reinforced Concrete, Columbia University, New York, 1991.

7. Thorenfeldt, E.; Tomaszewicz, A.; and Jensen, J. J., "Mechanical Properties of High-Strength Concrete and Application in Design," *Proceedings,* Symposium on Utilization of High-Strength Concrete, Stavanger, Norway, Tapir Trondheim, 1987.

8. Vecchio, F. J., "Nonlinear Finite Element Analysis of Reinforced Concrete Membranes," *ACI Structural Journal,* V. 86, No. 1, Jan.-Feb. 1989, pp. 26-35.